

# SUSY Monojets and Precision Coupling Determinations

Howard E. Haber

TH-LPCC Summer Institute on LHC Physics

23 August 2011

## Outline

- Introduction—the significance of the gaugino–quark–squark couplings
- Measuring the  $q\tilde{q}\tilde{\chi}_1^0$  coupling using LHC monojets
- An analytic study of the Jacobian peak
- The wino-LSP: a case study
- Conclusions and future directions

This talk is based on work that appears in: B.C. Allanach, S. Grab and H.E. Haber, “Supersymmetric Monojets at the Large Hadron Collider,” JHEP **1101** (2011) 138 [arXiv:1010.4261 [hep-ph]].

## Introduction—telltale signs of SUSY

Suppose that new physics beyond the Standard Model (SM) is discovered at the LHC. How will we know that it is SUSY (taking into account that SUSY is a broken symmetry)?

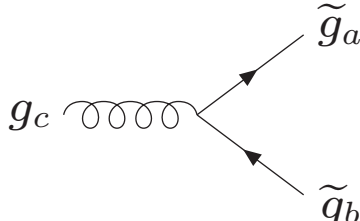
- Every SM particle has a superpartner differing in spin by half a unit.
  - You may only discover a subset of all the superpartners.
  - Spin measurements may be difficult in some cases.
- The total number of bosonic and fermionic degrees of freedom must be equal.
  - It is very unlikely that all MSSM degrees of freedom can be accessed at the LHC.

Perhaps the “gluino” that was discovered is an ordinary color octet fermion.

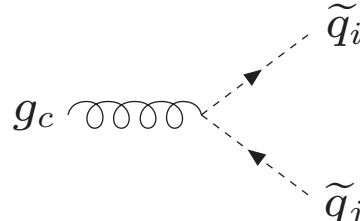
Perhaps the “squark” is an ordinary color triplet scalar.

## Fingerprints of SUSY—Yukawa couplings related to gauge couplings

Example: gluino and squark couplings

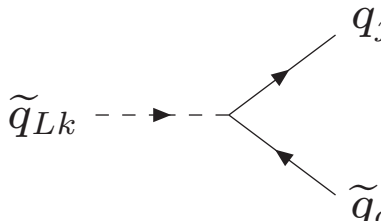


$$-g_s f^{abc} \gamma^\mu$$

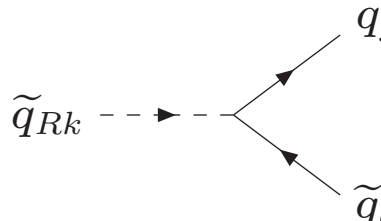


$$-i g_s T_{ij}^c (p_i + p_j)^\mu$$

These vertices are governed solely by QCD. In contrast, the  $\tilde{q}q\tilde{g}$  coupling is a scalar–scalar–fermion (Yukawa) coupling. In general, Yukawa and gauge interactions are unrelated. But, here it is the underlying supersymmetry that relates them.



$$-\frac{i g_s}{\sqrt{2}} T_{jk}^a (1 + \gamma_5)$$



$$\frac{i g_s}{\sqrt{2}} T_{jk}^a (1 - \gamma_5)$$

SUSY requires that these Yukawa couplings are proportional to the gauge coupling  $g_s$ .

## Testing SUSY coupling relations at colliders

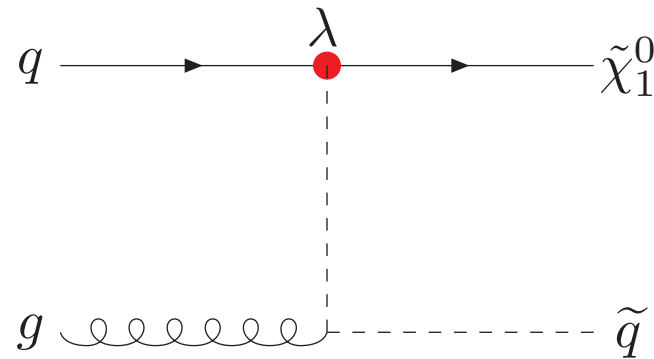
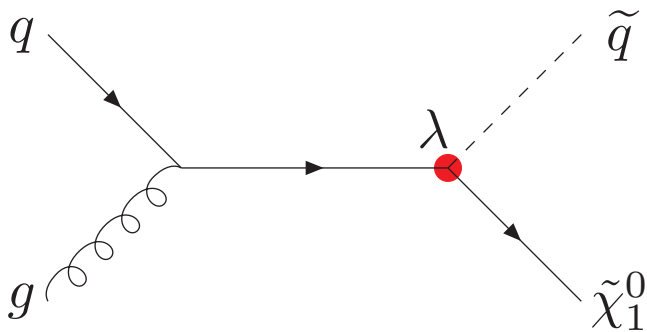
To verify coupling relations requires a precision SUSY program. This is *not* a program for early LHC running.

Suppose that after years of LHC running, a spectrum of new particles is discovered that is suggestive of SUSY. One might first try to verify the relation of the  $\tilde{q}q\tilde{g}$  coupling to the strong gauge coupling. A study by Freitas, Skands, Spria and Zerwas [JHEP **0707**, 025 (2007)] demonstrated the feasibility of this measurement, although with some SUSY model dependence and reliance on ILC data.

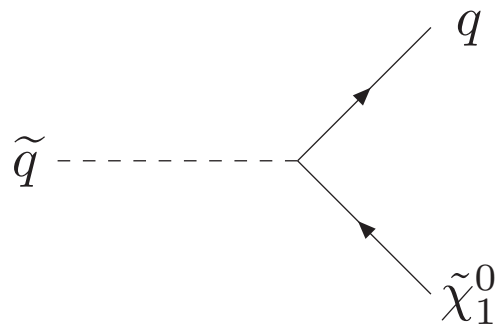
Instead, we propose to go after the SUSY coupling relations involving the lightest supersymmetric particle (LSP), assumed to be the  $\tilde{\chi}_1^0$ .

# Measuring the $\tilde{q}q\tilde{\chi}_1^0$ coupling using LHC monojet events

The production process involves the  $\tilde{q}q\tilde{\chi}_1^0$  coupling,  $\lambda$ . If the  $\tilde{\chi}_1^0$  is dominantly gaugino-like, then this coupling is directly related to the gauge coupling due to SUSY.



If the squark is lighter than the gluino, the squark will often decay directly to the LSP, resulting in a quark jet plus missing energy, i.e. a monojet event.



## The Jacobian peak in the $p_T$ distribution

Consider the  $2 \rightarrow 3$  partonic scattering process,

$$q + g \rightarrow \tilde{q} + \tilde{\chi}_1^0, \quad \text{followed by} \quad \tilde{q} \rightarrow q + \tilde{\chi}_1^0,$$

The quarks and gluon are treated as massless. The squark and neutralino masses are denoted by  $M$  and  $m$ , respectively. In the center-of-mass frame, the four-momenta of the initial quark and gluon and the final state quark jet are denoted by  $p_a$ ,  $p_b$  and  $p_1$ , where

$$p_a = \frac{1}{2}\sqrt{s}(1; 0, 0, 1), \quad p_b = \frac{1}{2}\sqrt{s}(1; 0, 0, -1),$$

$$p_1 = (E_1; p_T, 0, p_{\parallel}), \quad \text{where } p_T = E_1 \sin \theta \text{ and } p_{\parallel} = E_1 \cos \theta,$$

and  $\sqrt{s}$  is the partonic center-of-mass energy. The relevant kinematic invariants are

$$t_1 \equiv (p_a - p_1)^2 = -\sqrt{s} \left[ E_1 \mp \sqrt{E_1^2 - p_T^2} \right], \quad t_2 \equiv (p_a - p_c)^2 = A_1 + A_2 \cos \phi,$$

$$s_1 = p_c^2 = (p_1 + p_2)^2 = M^2, \quad s_2 \equiv (p_a + p_b - p_1)^2 = s - 2\sqrt{s}E_1,$$

where  $\phi$  is the azimuthal angle in the particle 2–3 rest frame between the plane spanned by  $\vec{p}_b$  and  $\vec{p}_1$  and the plane spanned by  $\vec{p}_1$  and  $\vec{p}_3$ , with  $\vec{p}_1$  as the axis.

The coefficients  $A_1$  and  $A_2$  are given by:

$$A_1 = m^2 - \frac{s_2(s - s_2 + t_1)(M^2 - m^2) - st_1(s - s_2 - M^2 + m^2)}{(s - s_2)^2},$$

$$A_2 = \frac{2 [st_1(s - s_2 + t_1)(M^4 s_2 - M^2 s_2(s - s_2 + 2m^2) + m^2 s(s - s_2) + s_2 m^4)]^{1/2}}{(s - s_2)^2}.$$

If  $C(s, t_2)$  is the scattering amplitude for the  $2 \rightarrow 2$  process,  $q + g \rightarrow \tilde{q} + \tilde{\chi}_1^0$ , then the differential cross-section for the partonic  $2 \rightarrow 3$  process is:

$$\frac{d\sigma}{ds_2 dt_1} = \frac{BM^2}{32\pi^2 s^2 (s - s_2)(M^2 - m^2)} \Theta\{-t_1(s + t_1 - s_2)\} \int_0^{2\pi} |C_1(s, A_1 + A_2 \cos \phi)|^2 d\phi,$$

where  $B \equiv \text{BR}(\tilde{q} \rightarrow q + \tilde{\chi}_1^0)$ . Changing variables from  $\{t_1, s_2\}$  to  $\{p_T^2, E_1\}$  involves a Jacobian. The kinematical limits of  $p_T$  and  $E_1$  are:

$$\text{for } 0 \leq p_T \leq E_1^-, \quad E_1^- \leq E_1 \leq E_1^+,$$

$$\text{for } E_1^- \leq p_T \leq E_1^+, \quad p_T \leq E_1 \leq E_1^+,$$

where

$$E_1^\pm \equiv \frac{M^2 - m^2}{4M^2 \sqrt{s}} \left[ s + M^2 - m^2 \pm \sqrt{(s + M^2 - m^2)^2 - 4sM^2} \right].$$

Introduce dimensionless variables,

$$w \equiv \frac{2E_1}{\sqrt{s}}, \quad x \equiv \frac{2p_T}{\sqrt{s}}, \quad y \equiv \frac{M^2}{s}, \quad z \equiv \frac{m^2}{M^2}.$$

Then the transverse momentum distribution is given by:

$$\frac{d\sigma}{dx} = \frac{Bx}{64\pi^2 s(1-z)} \int_{w_{\min}}^{w^+} \frac{dw}{w} \frac{1}{\sqrt{w^2 - x^2}} \int_0^{2\pi} d\phi \sum_{j=\pm} |C_1(s, A_1^{(j)} + A_2 \cos \phi)|^2$$

where  $w^\pm \equiv \frac{1}{2}(1-z) \left[ 1 + y(1-z) \pm \sqrt{(1+y-yz)^2 - 4y} \right],$

$$w_{\min} = \begin{cases} w^-, & \text{for } 0 \leq x \leq w^-, \\ x, & \text{for } w^- \leq x \leq w^+, \end{cases}$$

and the coefficients  $A_1^{(\pm)}$  and  $A_2$  are given by:

$$A_1^{(\pm)} = \frac{1}{2}s \left\{ y(1+z) - 1 \pm \frac{\sqrt{w^2 - x^2} [w + y(1-z)(w-2)]}{w^2} \right\},$$

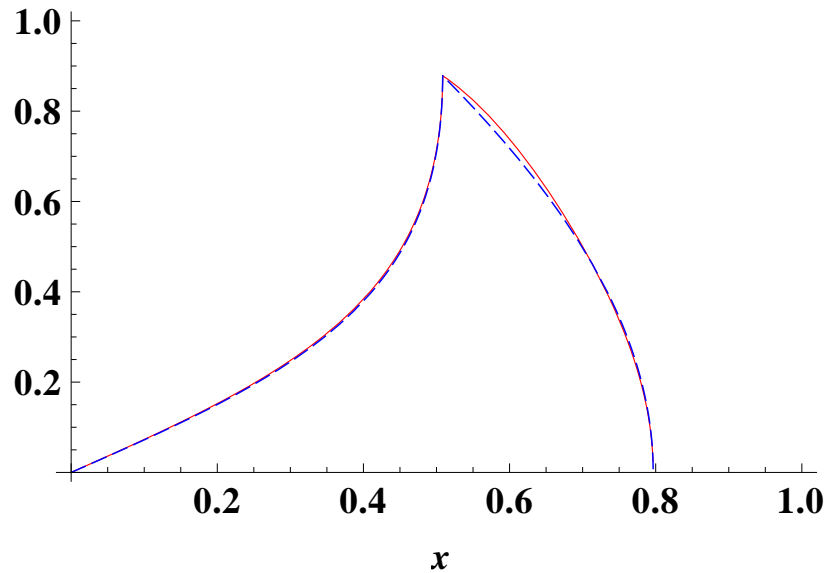
$$A_2 = \frac{sx y^{1/2}}{w^2} \left[ w(1-w-z) - y(1-w)(1-z)^2 \right]^{1/2}.$$



For  $C_1 = 1$  (pure phase space), the integral over  $E_1$  can be carried out explicitly,

$$\frac{d\sigma}{dx} = \frac{B}{16\pi s(1-z)} \left[ \tan^{-1} \left( \frac{\sqrt{[w^+]^2 - x^2}}{x} \right) - \Theta(w^- - x) \tan^{-1} \left( \frac{\sqrt{[w^-]^2 - x^2}}{x} \right) \right].$$

Employing the actual  $qg \rightarrow \tilde{q}\tilde{\chi}_1^0$  matrix element  $C_1$  yields only a small correction to the shape of the  $p_T$  distribution. Note that  $x_{\text{peak}} = w^-$  and  $x_{\text{max}} = 2(p_T)_{\text{max}}/\sqrt{s} \leq w^+$ .



Unnormalized cross-section as a function of  $x \equiv 2p_T/\sqrt{s}$  for  $qg \rightarrow \tilde{q}\tilde{\chi}_1^0 \rightarrow q\tilde{\chi}_1^0\tilde{\chi}_1^0$ , (solid curve), assuming  $M_{\tilde{q}}^2 = 0.5s$  and  $m_{\tilde{\chi}}^2 = 0.1M_{\tilde{q}}^2$  (i.e.,  $y = 0.5$  and  $z = 0.1$ ). In this example,  $x_{\text{peak}} = 0.508$  and  $x_{\text{max}} = 0.797$ . If the matrix element for  $qg \rightarrow \tilde{q}\tilde{\chi}_1^0$  is set equal to unity, one obtains the dashed curve. The relative normalization of the two curves has been fixed such that the height of the peaks of the distributions coincide.

The location of the Jacobian peak depends on the partonic center-of-mass energy  $\sqrt{s}$ . To compute  $d\sigma/dp_T(pp \rightarrow \tilde{q}\tilde{\chi}_1^0 \rightarrow q\tilde{\chi}_1^0\tilde{\chi}_1^0)$ , one must integrate over the parton distribution functions. The dominant contribution arises close to threshold, where  $\sqrt{s} = M + m$ , which yields

$$E_1^- = E_1^+ = \frac{M^2 - m^2}{2M}.$$

Thus, close to threshold,

$$(p_T)_{\text{peak}} = E_1^- \simeq \frac{M^2 - m^2}{2M}$$

which is independent of the partonic center-of-mass energy.

As  $\sqrt{s}$  is increased above the threshold energy, the value of  $E_1^-$  *decreases* relative to the above estimate. Thus, we expect the actual peak in the transverse momentum distribution of the hadronic scattering process (or equivalently in the missing transverse energy distribution) to be broader with a maximum that is less than the above result.

## Details of the signal process

The phenomenology of the signal depends on the properties of the LSP. In this study, we focus on a wino LSP, which arises in anomaly mediated SUSY-breaking models. In this case,  $\{\tilde{\chi}_1^0, \tilde{\chi}_1^\pm\}$  comprise a nearly mass-degenerate  $SU(2)_L$  triplet.

The partonic scattering processes that yield monojet events are:  $g + u \rightarrow \tilde{\chi}_1^0 + \tilde{u}_L$ ,  $g + d \rightarrow \tilde{\chi}_1^0 + \tilde{d}_L$ ,  $g + u \rightarrow \tilde{\chi}_1^+ + \tilde{d}_L$ ,  $g + d \rightarrow \tilde{\chi}_1^- + \tilde{u}_L$ , plus the charge-conjugated processes, where  $\tilde{u}_L \rightarrow u\tilde{\chi}_1^0/d\tilde{\chi}_1^+$ ,  $\tilde{d}_L \rightarrow d\tilde{\chi}_1^0/u\tilde{\chi}_1^-$  and  $\tilde{\chi}_1^+ \rightarrow S + \tilde{\chi}_1^0$  ( $S$  is either a very soft lepton or QCD radiation too soft to be identified as a jet). Here,  $\lambda = g$ , the  $SU(2)_L$  gauge coupling.

- The mass splitting between  $\tilde{\chi}_1^+$  and  $\tilde{\chi}_1^0$  is  $\sim 200$  MeV, so the dominant decay  $\tilde{\chi}_1^+ \rightarrow \tilde{\chi}_1^0\pi^+$  typically results in an unmeasurable soft pion.
- Since  $\tilde{q}_L$  is an  $SU(2)_L$ -triplet, there is a preference for the direct decay of  $\tilde{q}_L \rightarrow q\tilde{\chi}_1^0$ .

## Significant SM and SUSY backgrounds

- $Z(\rightarrow \nu \bar{\nu}) + \text{jet}$ . This background can be ascertained from the  $Z(\rightarrow \ell^+ \ell^-) + \text{jet}$  signal. In principle, this background can be subtracted off from the monojet sample.
- $W(\rightarrow \tau \nu) + \text{jet}$ , where the  $W$  decays into a tau and a neutrino, and the tau is either not detected, or lost in the jet.
- $W(\rightarrow e/\mu \nu) + \text{jet}$ , where the  $W$  decays into an electron or a muon and a neutrino and the electron/muon is undetected or lost inside the jet.
- QCD jet production with mismeasurement of the energy deposited in the detector. One could produce di-jets, for instance, and one of the jets could be lost in the detector (or its energy mismeasured so that it fluctuate below the transverse momentum required to identify the jet).
- $\tilde{q}\tilde{q}$  production, where the decay products of the two squarks merge into a single jet.
- $\tilde{\chi}_1^0 \tilde{\chi}_1^0$  production plus an initial state radiated (ISR) jet.
- In the case of a wino LSP,  $\tilde{\chi}_1^+ \tilde{\chi}_1^-$  production plus an ISR jet will yield monojet events, since  $\tilde{\chi}_1^+ \rightarrow \tilde{\chi}_1^0 + \text{soft pion}$ .

# Simulation of signal and backgrounds

The following tools have been employed:

- Herwig++2.4.2
  - signal and backgrounds at tree-level have been simulated
  - pair production and the two and three body decay of all SUSY particles included
- Herwig++ output analyzed using HepMC-2.04.02 and ROOT
- Jets were reconstructed using fastjet-2.4.1
  - Jets are defined with  $p_T > 30$  GeV, and the anti- $k_t$  jet algorithm with  $R \equiv \sqrt{(\Delta\eta)^2 + (\Delta\phi)^2} = 0.7$  was used.
- SUSY spectrum determined with SOFTSUSY3.0.13

## Wino-LSP case study

We examine the benchmark mAMSB scenario with:

$$M_{3/2} = 33 \text{ TeV}, \quad M_0 = 200 \text{ GeV}, \quad \tan \beta = 10, \quad \text{sgn}(\mu) = +1,$$

which gives  $\sigma(pp \rightarrow \tilde{q}_R \tilde{\chi}_1^0) = 470 \text{ fb}$ ,  $\lambda = 0.99g$  and the following SUSY spectrum:

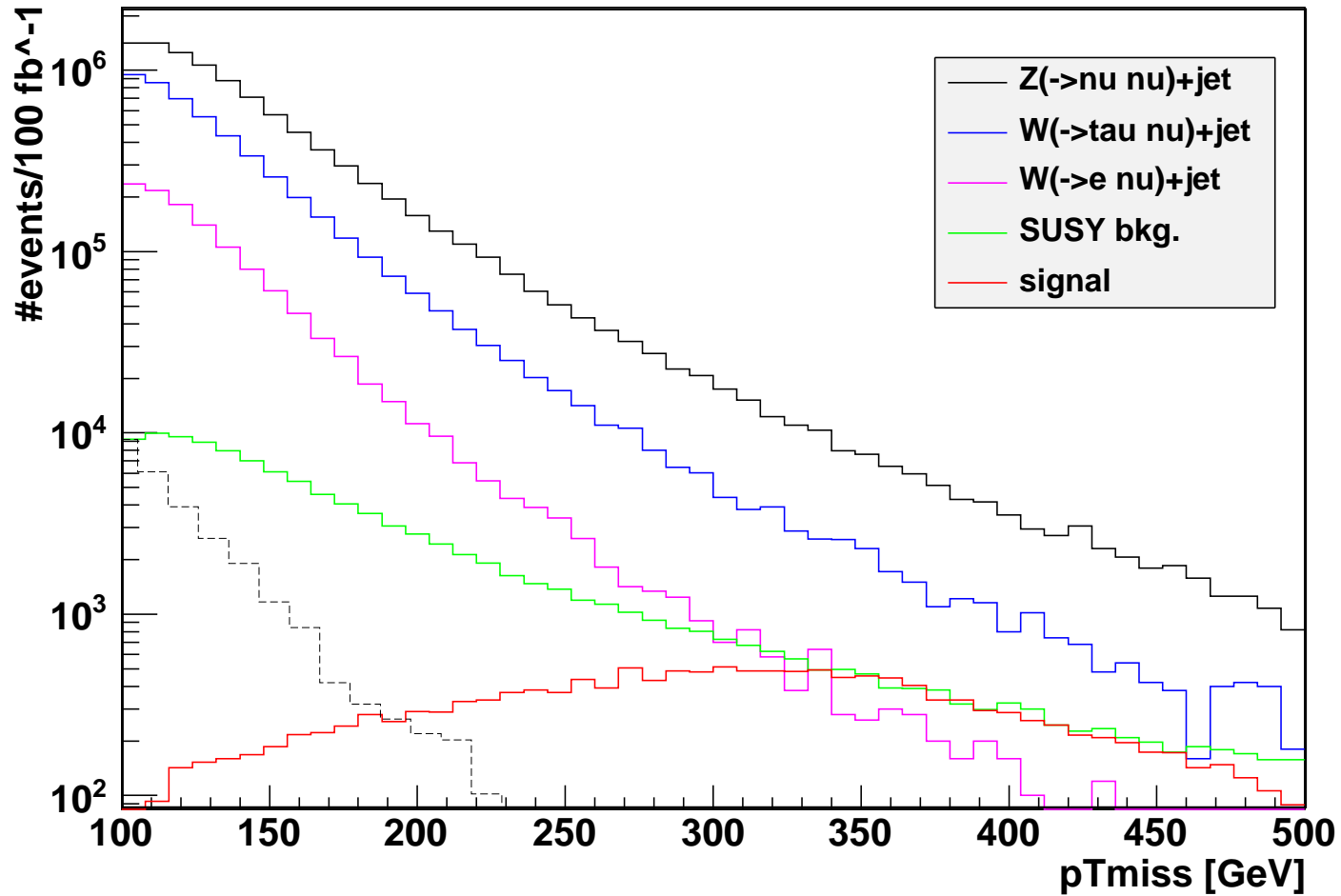
sparticle	mass [GeV]	sparticle	mass [GeV]
$\tilde{\chi}_1^0$	106.5	$\tilde{\chi}_4^0$	593
$\tilde{\chi}_1^+$	106.7	$\tilde{\chi}_2^+$	594
$\tilde{\tau}_1$	113	$\tilde{b}_1$	634
$\tilde{\nu}_\tau$	135	$\tilde{t}_2$	688
$\tilde{\nu}_e/\tilde{\nu}_\mu$	138	$\tilde{u}_L/\tilde{c}_L$	722
$\tilde{e}_R/\tilde{\mu}_R$	150	$\tilde{b}_2$	723
$\tilde{e}_L/\tilde{\mu}_L$	159	$\tilde{d}_L/\tilde{s}_L$	726
$\tilde{\tau}_2$	179	$\tilde{u}_R/\tilde{c}_R$	726
$\tilde{\chi}_2^0$	298	$\tilde{d}_R/\tilde{s}_R$	732
$\tilde{t}_1$	521	$\tilde{g}$	745
$\tilde{\chi}_3^0$	584		

The cuts employed in our analysis are summarized below, based on an integrated luminosity of  $100 \text{ fb}^{-1}$  at  $\sqrt{s} = 14 \text{ TeV}$ .

cut	all SM	SUSY bkg.	signal	$S/\sqrt{B}$ ( $S/\sqrt{7B}$ )
$p_T(\text{jet1}), \cancel{p}_T > 100 \text{ GeV}$	$3.81 \times 10^7$	$1.04 \times 10^6$	44 100	-
lepton veto	$2.52 \times 10^7$	621 000	43 800	-
$p_T(\text{jet2}) < 50 \text{ GeV}$	$1.73 \times 10^7$	111 000	16 200	3.9 (1.5)
$\cancel{p}_T > 300 \text{ GeV}$	171 000	11 000	8 390	20 (7.7)
$m(\text{jet1}) < 80 \text{ GeV}$	135 000	6 020	6 370	17 (6.5)
tau veto	119 000	5 840	6 370	18 (7.0)
$b$ -jet veto	115 000	5 290	6 320	19 (7.0)

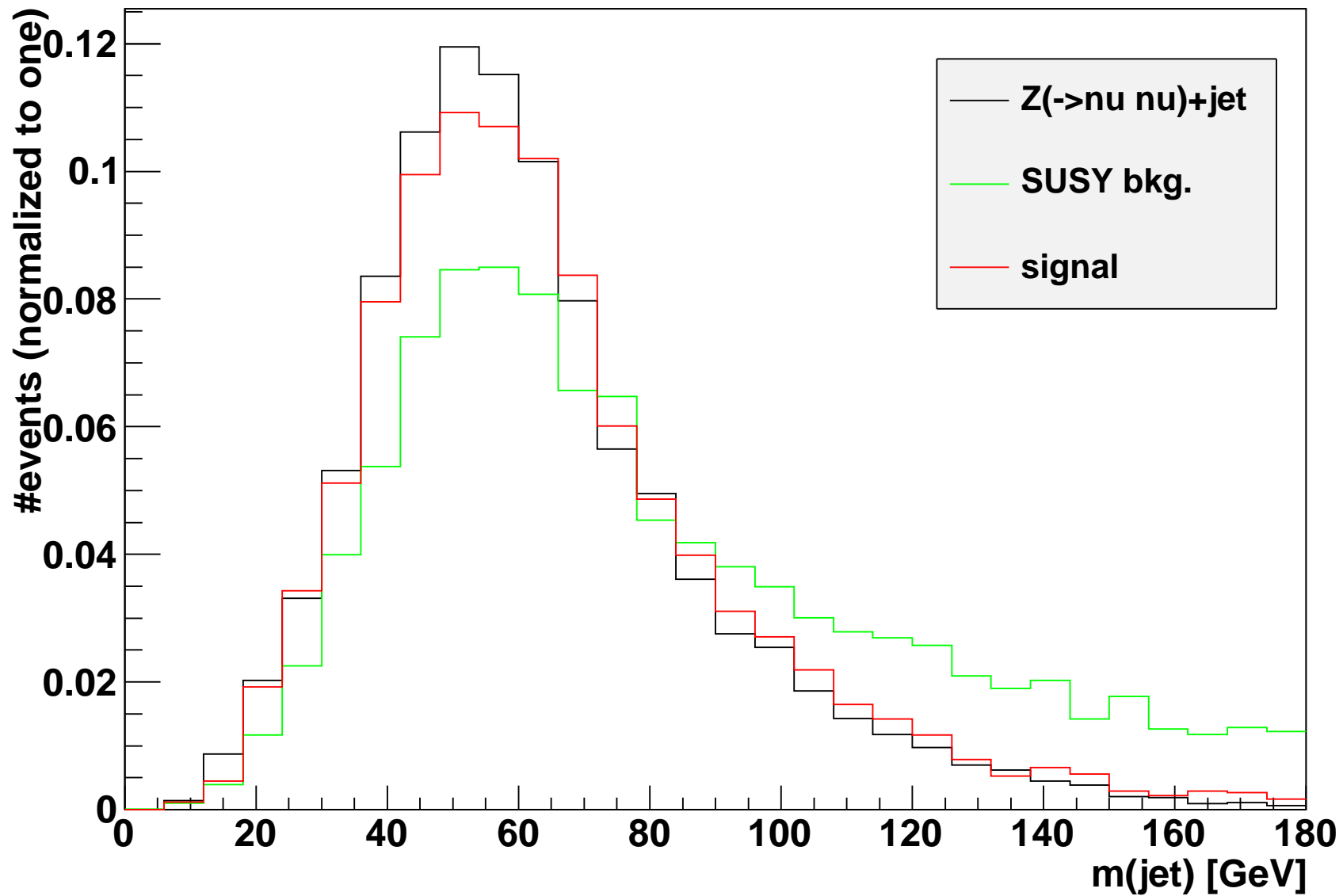
The lepton veto removes events with an isolated electron or muon with  $p_T > 5 \text{ GeV}$  and  $|\eta| < 2.5$ . The isolation criterion demands  $\leq 10 \text{ GeV}$  of additional energy in a cone of radius  $\Delta R = 0.2$ . The conservative statistical estimator  $S/\sqrt{7B}$  should be used (according to L. Vacavant and I. Hinchliffe) if statistical fluctuations are dominated by the  $Z(\rightarrow \ell^+ \ell^-) + \text{jet}$  calibration sample used to subtract the  $Z(\rightarrow \nu \bar{\nu}) + \text{jet}$  background.

Note that we need a good signal to SUSY background if we wish to measure the  $\tilde{q}q\tilde{\chi}_1^0$  coupling  $\lambda$  to good precision. This is the main reason for the cut on  $m(\text{jet1})$ . The  $\tau$  and  $b$ -jet vetoes are not used in our final analysis.



The QCD background is shown as a black dashed histogram. The first three cuts listed in the previous table have been applied. The signal exhibits a Jacobian peak, whose position depends on the  $\tilde{q}$  and  $\tilde{\chi}_1^0$  masses.





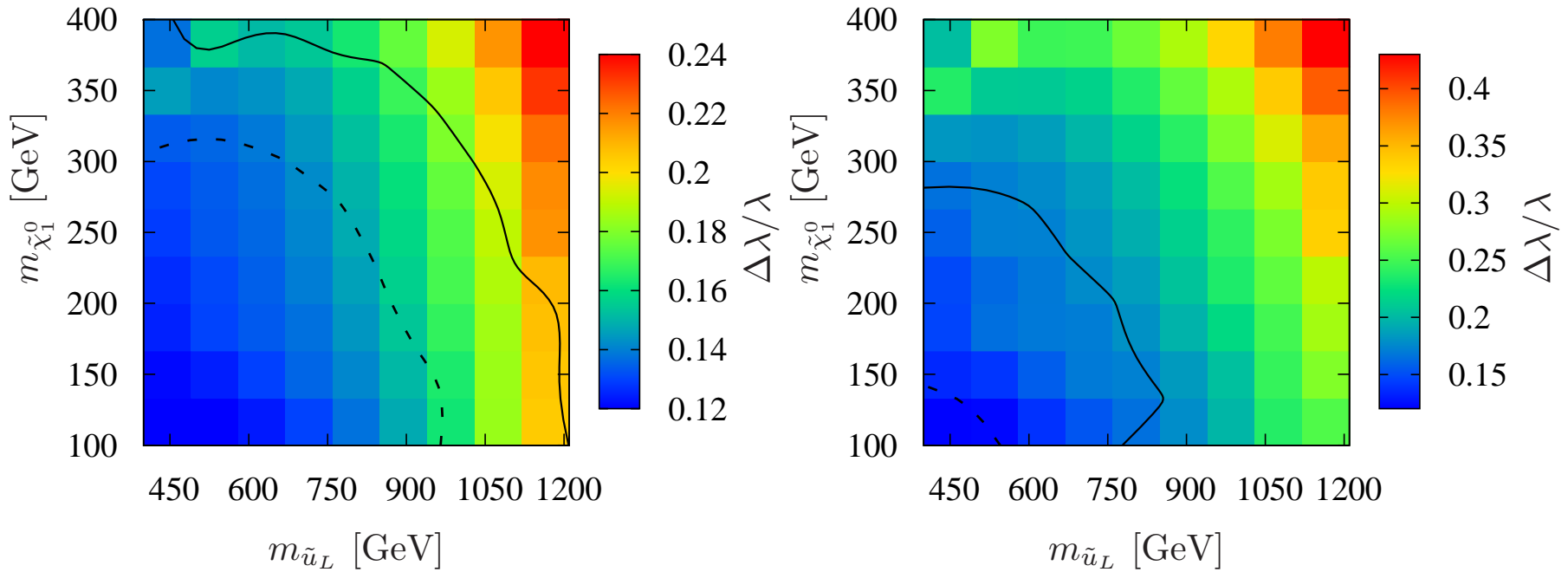
The invariant mass distribution of the hardest jet, normalized to one. The first four cuts listed in the previous table have been applied. The QCD background has a distribution almost indistinguishable from that of  $Z(\rightarrow \nu \bar{\nu}) + \text{jet}$ .

## Accuracy in the determination of the $\tilde{q}q\tilde{\chi}_1^0$ coupling $\lambda$ in the wino case study

error	$\Delta\sigma_{\text{mono}}/\sigma_{\text{mono}}$	$\Delta\lambda/\lambda$
luminosity	3%	1.5%
PDF uncertainty	17%	8.3%
NLO corrections	18%	9%
sparticle mass $\Delta\tilde{m} = 10$ GeV	7.3%	3.7%
statistics (optimistic)	5.8%	2.9%
statistics (conservative)	15%	7.7%
total (optimistic)	26%	13%
total (conservative)	30%	15%

Relative errors for the signal monojet cross section (second column) and the  $\tilde{q}_Lq\tilde{\chi}_1^0$  coupling (third column) from different sources (first column). The numbers are for the mAMSB benchmark scenario.

An optimal choice of cuts depends on the squark and neutralino mass. We searched in steps of 10 GeV for the  $p_T$  and  $m(\text{jet1})$  cuts that provide the highest  $S/\sqrt{S+B}$ . The best significance is near the Jacobian peak. Applying these optimal cuts yields:



Fractional precision to which the  $\tilde{q}_L q \tilde{\chi}_1^0$  coupling  $\lambda$  can be reconstructed as function of the squark and  $\tilde{\chi}_1^0$  mass. The left (right) figure employs our optimistic (conservative) estimate for the SM background uncertainties. The solid and dashed black lines correspond to  $S/\sqrt{B}$  ( $S/\sqrt{7B}$ ) of  $5\sigma$  and  $10\sigma$ , respectively.

## Conclusions and future directions

- For a wino-LSP, one can test the  $\tilde{q}q\tilde{\chi}_1^0$  coupling relation to a precision of  $\sim 10\%$ — $20\%$  at the LHC with  $\sqrt{s} = 14$  TeV and  $100 \text{ fb}^{-1}$  using monojet events if squark masses are below 1 TeV, over a significant portion of the wino-LSP parameter space.
- For a bino-LSP or higgsino-LSP, the monojet events at the LHC cannot be used for precision coupling measurements due to a significantly weaker quark–squark neutralino coupling strength.
- In the future, one must examine multiple SUSY observables at the LHC that are sensitive to the gaugino–particle–sparticle coupling. A global fit to these observables can enhance the precision of the coupling determinations, while providing stronger evidence in favor of the underlying SUSY structure.